

## Refining Reaction Dynamics in Fermi Energy Heavy Ion Reactions

R.Wada, Z. Chen, T. Keutgen, K. Hagel, J. Wang, L. May, M. Codrington, L. Qin,  
J.B. Natowitz, T. Materna, S. Kowalski, and P.K. Sahu

In heavy ion reactions in the Fermi energy domain, many intermediate mass fragments (IMFs) are commonly produced. At a time of formation their characteristic properties, such as the excitation energy and isotope distributions, are governed by the physical nature of the source, such as temperature, density and N/Z ratio, from which they originate. These physical conditions of the sources are directly related to the reaction dynamics and the nature of nuclear matter. Therefore IMFs may provide a unique probe to study reaction mechanism and nuclear properties. However most of IMFs experimentally measured are not direct reaction products (primary IMFs) , but they are secondary products produced through sequential cooling processes. These secondary decay processes may significantly distort the characteristics of the primary IMFs and obscure the physical nature of the source. Therefore it is desirable to reconstruct the characteristics of the primary fragments in order to extract the physical natures of the sources and to refine the reaction dynamics.

Aiming at this goal, reaction systems with different N/Z ratios have been studied. In the experiment  $^{64}\text{Zn}$ ,  $^{64}\text{Ni}$  and  $^{70}\text{Zn}$  beams were incident on  $^{58}\text{Ni}$ ,  $^{64}\text{Ni}$ ,  $^{112}\text{Sn}$ ,  $^{124}\text{Sn}$ ,  $^{197}\text{Au}$  and  $^{232}\text{Th}$  targets at 40 A MeV. In order to reconstruct the primary IMFs, neutron and charged particles are detected in coincidence with IMFs. In this report we concentrate on the light particles. Another brief report for the analysis of the IMFs is given in a separate article in this annual report.

Neutrons were detected by sixteen detectors from the Belgian-French neutron detection array, DEMON. Light Charged particles (LCPs) were detected by 16 single crystal CsI(Tl) detectors. Both particles were recorded in coincidence with IMF observed at  $20^\circ$ . Neutron- $\gamma$  separation and charged particle identification were made by pulse shape discrimination methods. Neutron energy is obtained from the time of flight measurement and the neutron detection threshold was calibrated by a  $^{22}\text{Na}$  source. The energy calibration of the CsI detector was performed using a Si detector in front of each CsI detector during the beam time.

In Figure 1, typical neutron velocity spectra associated with  $^6\text{Li}$  of different velocity are shown. Neutrons in coincidence with  $^6\text{Li}$  in three different velocity windows,  $V_{6\text{Li}} \leq 4.5\text{cm/ns}$ ,  $5.5\text{cm/ns} \leq V_{6\text{Li}} \leq 6.5\text{cm/ns}$  and  $6.5\text{cm/ns} \leq V_{6\text{Li}} \leq 7.5\text{cm/ns}$  are presented from top to bottom, respectively. spectra at different neutron detection angles are shown from left to right. The angles indicated on the top of each row are the opening angle,  $\theta_{\text{IMF-N}}$ , between the Si telescope ( $\theta=20^\circ$ ) and the demon detectors. In this plot neutrons are detected in perpendicular to the reaction plane determined by the Si telescope and the beam. Neutron spectra associated with  $^6\text{Li}$  in the velocity window of  $4.5\text{cm/ns} \leq V_{6\text{Li}} \leq 5.5\text{cm/ns}$ , which is tentatively used as a reference, are shown by dashed line histograms in each spectra . As seen in the figure, no significant differences from the reference spectra are observed in shape and amplitude at different angles and for different IMF velocity windows. This indicates that there are very few excess neutrons focused along the direction of IMF, indicating that a very small amount of neutrons are emitted directly from the parent nuclei of the detected  $^6\text{Li}$  isotopes. A similar observation has been made in our

previous work in which the charged particle multiplicities associated with IMFs are extracted in the Xe+Sn reaction at 50 AMeV[1].

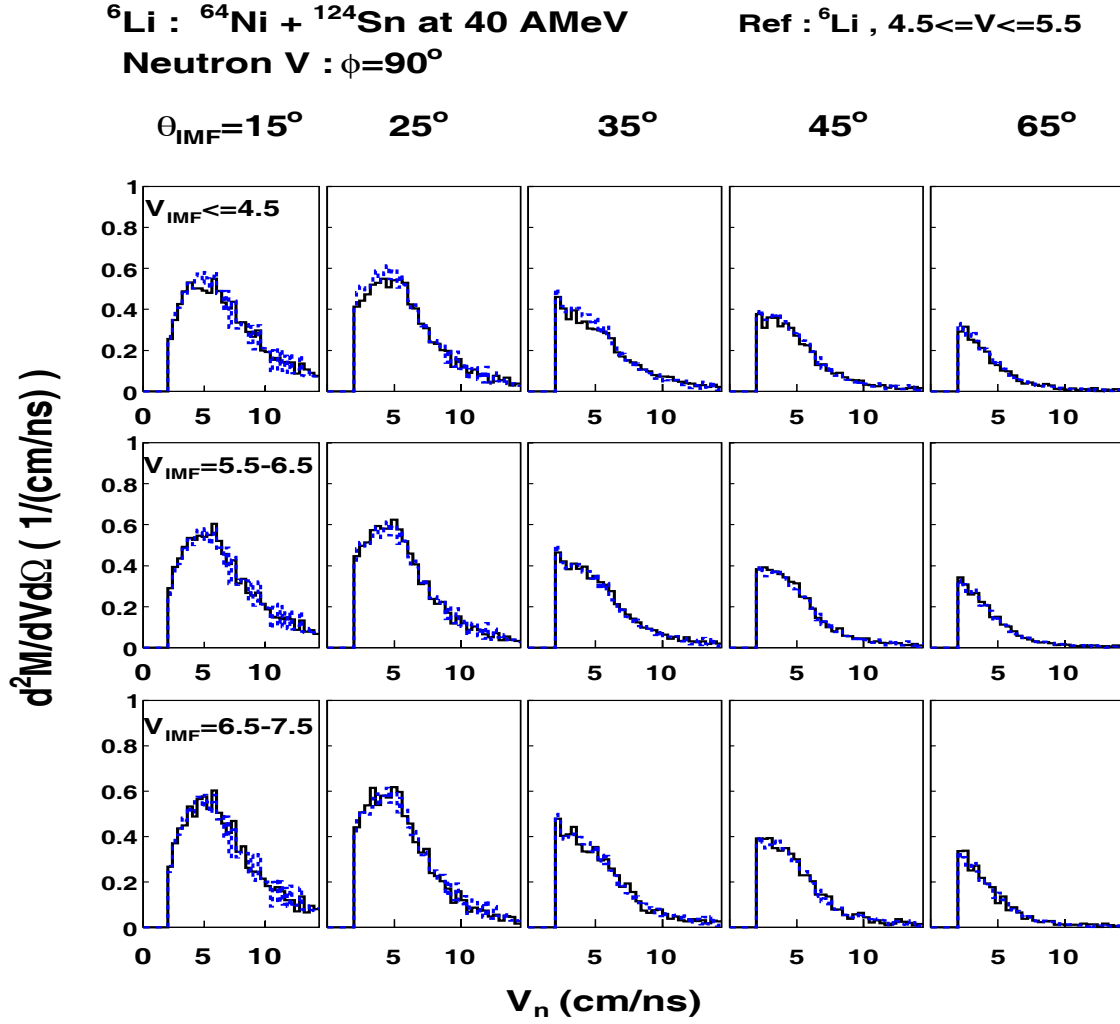


**Figure 1.** Neutron velocity spectra observed at different angles in coincidence with  ${}^6\text{Li}$  in different velocity windows for  ${}^{64}\text{Ni}+{}^{124}\text{Sn}$ . See details in the text.

In Figure 2 a similar plot is shown for neutrons associated with  ${}^{18}\text{O}$ . Comparing to the reference spectra, a notable excess of neutrons is observed, especially at small angles,  $\theta_{\text{IMF-N}}$ . In the lowest velocity window of  ${}^{18}\text{O}$  (top row), these excess neutrons are distributed in a wider range of  $\theta_{\text{IMF-N}}$ . The peak position of the excess neutrons at  $\theta_{\text{IMF-N}}=15^\circ$  shifts toward the higher velocity side when the IMF velocity becomes higher. These observations strongly indicate that these excess neutrons originate from the parent nuclei of the detected  ${}^{18}\text{O}$ , reflecting the kinematic focusing of neutrons along the direction of IMFs. For a higher velocity of  ${}^{18}\text{O}$  (bottom row), the kinematical focussing becomes stronger and at the velocity window of  $7.5 \text{ cm/ns} \leq V_{{}^{18}\text{O}} \leq 8.5 \text{ cm/ns}$  the excess is only observed at  $\theta_{\text{IMF-N}}=15^\circ$ . At larger angles a small depletion of neutrons is observed on the higher velocity side. A similar effect is also observed for the charged particle velocity spectra.

In order to reconstruct the characteristic properties of the primary IMFs, a further quantitative analysis is now underway.

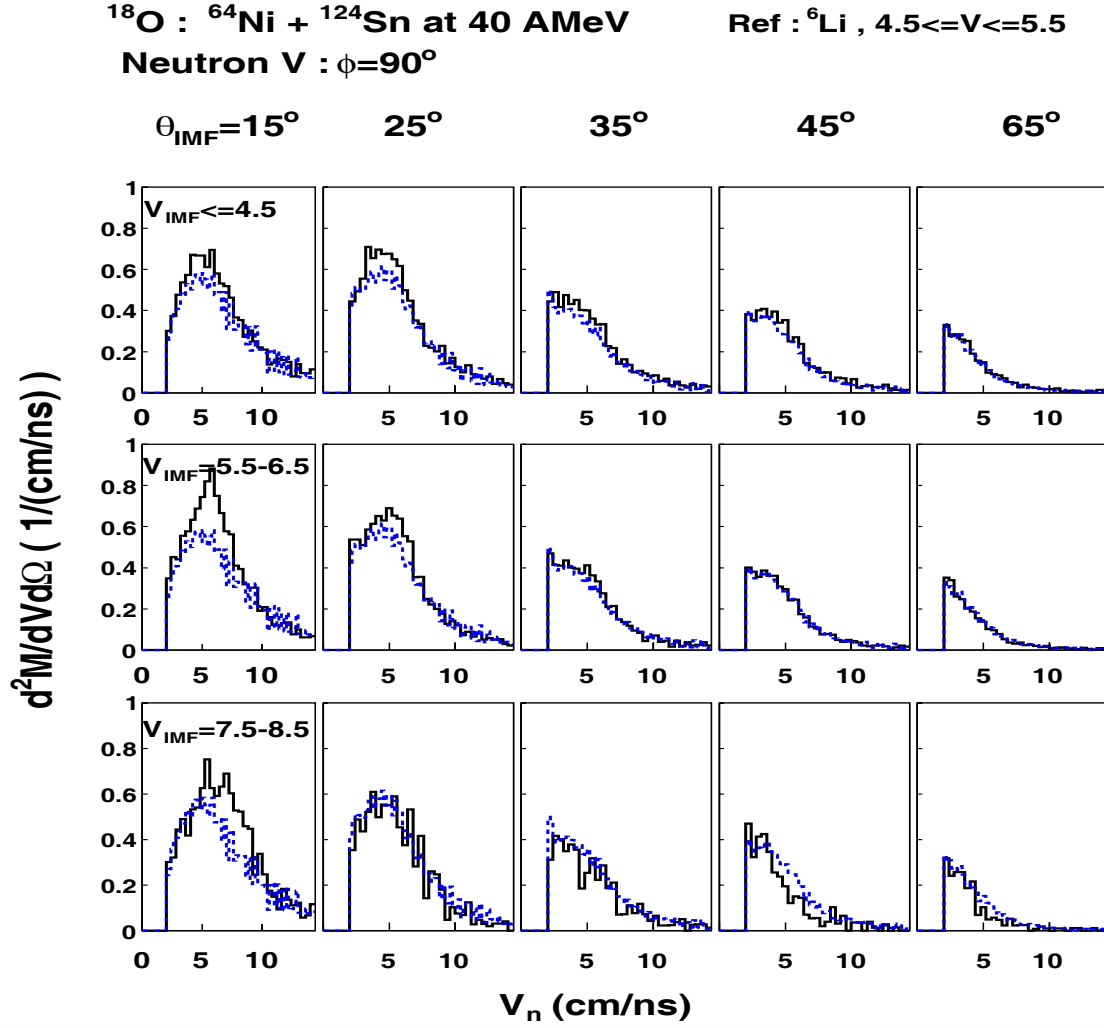


**Figure 2.** Similar neutron spectra to Fig.1, but in coincidence with  $^{18}\text{O}$ .

[1] N. Marie *et al.*, Phys. Rev. C **58**,256 (1998).